Enhanced osteogenesis of stem cells using poly (L-lactide-co-D, L-lactide)/poly (vinyl alcohol) nanofibrous scaffolds reinforced by Phospho- calcified cellulous nanowhiskers

Pejman Ghaffari-Bohlouli[a], Hafez Jafari[b], Alireza Khatibi[a], Mamak Bakhtiari[a], Beeta Tavana[a], Payam Zahedi[a,*], Amin Shavandi[b,*]

[a] *Nano-Biopolymers Research Laboratory, School of Chemical Engineering, College of Engineering, University of Tehran, P.O. Box: 11155-4563, Tehran, Iran*

[b] *BioMatter Unit—BTL, École Polytechnique de Bruxelles, Université Libre de Bruxelles, Avenue F.D. Roosevelt, 50-CP 165/61, Brussels 1050, Belgium*

[*] **To whom correspondence should be addressed:**

Email: phdzahedi@ut.ac.ir (P. Zahedi)

Tel: +98 (21) 61112247

Fax: +98 (21) 66957784

Co-correspondence:

Email: Amin.Shavandi@ulb.be

Abstract

This work aim is to develop hydrophilic and biodegradable nanofibrous scaffolds for bone tissue engineering based on poly (L-lactide-co-D, L-lactide) (PLDLLA) and poly (vinyl alcohol) (PVA) reinforced by phospho-calcified cellulose nanowhiskers (PCCNWs). PCCNWs with inherent hydrophilic properties enhanced the mechanical properties, hydrophilicity and hydrolytic degradation of the nanofibrous. Moreover, calcium phosphate and phosphate functional groups on the surface of PCCNWs possessing act as stimulating agents for cellular activities such as proliferation and differentiation. The Physico-chemical properties of nanofibrous samples including functional groups, contact angle, water up-take, hydrolytic degradation, and tensile properties were measured. The cytotoxicity of PLDLLA/PVA-PCCNWs nanofibrous samples was studied by MTT assay and did not show any toxicity for all nanofibrous samples. Incorporated 1 wt.% of PCCNWs into the PLDLLA/PVA nanofibrous sample showed more enzymatic activities and deposited calcium that were evaluated by Alkaline phosphatase assay (ALP), and calcium content and Alizarin red staining, respectively compared to other samples with 0, 0.1, and 0.5 wt.% of PCCNWs. The micrograph FE-SEM images of the morphology of human mesenchymal stem cells (hMSCs) cultured on nanofibrous samples after 14 days of cell differentiation showed samples containing PCCNWs had a good potential for bone tissue engineering.

Keywords: Poly (L-lactide-co-D, L-lactide); Poly (vinyl alcohol); cellulose nano whiskers; nanofibers; bone tissue engineering.

1 Introduction

While bone is able to rebuild itself in the case of minor fractures and cracks, in case of sever damages it cannot fully recover [1]. An ideal scaffolds for bone tissue engineering should be biocompatibile, biodegradable, with high porosity, good mechanical properties, and hydrophilic [1-3]. Biopolymer based scaffolds have been widely researched for application in bone tissue engineering because of their excellent features, availability, tunable properties, and good processability [2]. Poly (lactic acid) [PLA] [1], polyurethane [PU][3], poly-(ε-caprolactone) [PCL][2], chitosan[4], gelatin[5], and keratin [6], etc., [7-9] are a few examples of bio-based synthetic and natural polymers that have been used in bone tissue engineering.

PLA is one of the most common synthetic biopolymers which has been extensively used for bone tissue engineering due to its high mechanical strength, biocompatibility, biodegradability, tunable properties, and good processability [1, 10]. To accelerate degradation rate of PLA, it has been modified via copolymerization of L-lactide and D, L-lactide isomers to produce poly (L-lactide-co-D, L-lactide) [PLDLLA][11]. Hence, flexibility and rate of degradation are improved in PLDLLA compared to PLA but it still does not meet required hydrophilicity for tissue engineering applications. Poly (vinyl alcohol) (PVA), collagen, gelatin, and poly (acrylic acid), which are hydrophil, were Blended and hybridized with PLA as effective methods for increasing hydrophilicity in PLA [1, 11-14]. As a result of poly (vinyl acetate) hydrolysis, PVA is obtained and its characteristics depend on the degree of hydrolysis of poly (vinyl acetate) [11]. PVA is renowned for its biocompatibility, chemical resistance and hydrophilicity, causing it to be a good choice for biomedical applications. However, crosslinking of PVA is necessary for using it in

the mentioned areas [11]. Blending PLDLLA with PVA is as an efficient approach to reduce hydrophobicity and slow degradation rate of PLDLLA. In a previous study [11], PLDLLA blended with PVA exhibited higher hydrophilicity compared to the PLDLLA.

In addition to hydrophilicity , bone scaffolds should possess good mechanical properties and high porosity [2, 3]. Reinforcing porous scaffolds with cellulose nanowhiskers (CNWs) with high elastic modulus, chemical reactivity, and high specific surface area (SSA) will enhance the mechanical properties of the scaffold [2, 3, 15]. Agro-industrial residues contain a huge amount of cellulose and since a large portion of wastepaper in the world is not being recycled, therefore researchers have done myriad studies on producing CNWs from wastepaper[2, 3]. The presence of functional groups such as hydroxyl, carboxyl, and carbonyl on CNWs provides the possibility of different surface modification which makes CNWs as a promising candidate in biomedical engineering [15]. Another vital trait of scaffolds for bone applications is to be able to perform like natural extra-cellular matrix (ECM) to enhance osteogenic differentiation [2, 15]. Evoking differentiation into bone cells and proliferation of stem cells in scaffolds by calcium phosphate groups we take advantage of functional groups on surface of CNWs and modified their surface with phosphate and calcium phosphate groups [15, 16]. Hence, can be concluded that calcium phosphate groups on CNWs (PCCNWs) enhanced the osteogenic differentiation of human stem cells (hMSCs) [15].

In this work, PLDLLA hydrophilicity and mechanical properties were improved via introducing of PVA and various percentage of PCCNWs (0-1% per PLDLLA weight), which could enhance the mechanical properties, hydrophilicity followed by cell adhesion, and osteogenic differentiation. Physico-chemical, morphological, mechanical, hydrophilicity, hydrolytic degradation, biocompatibility, cell viability, and cell adhesion, as well as the hMSCs differentiation on nanofiber composite scaffold were investigated.

Commented [AS1]: I will revise it later

Commented [AS2]: this is out of nowhere

2 Experimental

2.1 Materials

Paper powder was purchased from the Linter Pak™ (Tehran, Iran), which were ground in the Linter Pak factory (Tehran, Iran). Phosphoric acid 85% (H_3PO_4-ortho), N, N-Dimethylformamide (DMF), and Dimethyl sulfoxide (DMSO), were obtained from the Merck Millipore (Darmstadt, Germany). Poly (L-lactide-CO-D, L-lactide) (PLDLLA) (a biological macromolecule of Resomer LR708 grade and average molecular weight of 1.5×10^6 Da, L-lactide: D, L-lactide ratio of 70:30,) was purchased from Evonik Industries (Germany). Poly (vinyl alcohol) (PVA) (a white-yellowish powder with an average molecular weight of 98,000 Da, and with the degree of hydrolysis ~88 mol%, trade name GH-17RGOHSENOL) was purchased from NIPPON GOHSEI Co.(Japan).

2.2 Preparation of PCCNWs

Cellulose nanwhiskers (CNWs) were prepared from wastepaper based on previous method [2, 15]. The soaked wastepaper fibers in distilled water were squeezed and dried at 40 ℃ for 24 h to enhance its dissolution in phosphoric acid. 190 mL of phosphoric acid 85 wt.% was used for the hydrolyzation of 10 g of the dried wastepaper fibers at 80 ℃ for 30 min under 1500 rpm agitation in a three-necked round bottom flask (500 mL). To terminate the reaction, 300 mL distilled water was added to the reaction media. The reacted wastepaper fibers with phosphoric acid were precipitated by centrifuged at 10000 rpm (G-force (RCF) of 11180 g) for 5 min. The precipitated substances were rinsed in 300 mL distilled water and centrifuged several times to reach a pH of 5. Then, dialysis was conducted for 3 days to achieve a pH of 5.5 to 6. The CNWs suspension was sonicated using an ultrasonic homogenizer at 19.5 kHz and 300 W with a probe tip diameter of 26 mm, US-300T, Nissei, Japan for 5 min. To achieve a pH of 7 for ultrasonicated CNWs, the suspension was neutralized by an equivalent amount of calcium hydroxide.

Neutralization was performed by increasing calcium hydroxide content until 2 mg. mL^{-1} concentration. Finally, the produced PCCNWs were stored in a refrigerator at 4 ℃ until when they were used.

2.3 Preparation of electrospun PLDLLA/PVA nanofibrous samples containing PCCNWs

To prepare the PLDLLA/PVA solution, firstly, PLDLLA and PVA were dissolved in DMF and DMSO, respectively, until a clear solution with 3.4% (w. v^{-1}) of PLDLLA and 3% (w. v^{-1}) of PVA were obtained. PVA solution and PLDLLA solution (3.4%) were mixed at a ratio of 1:9 and continuously stirred at room temperature to reach a homogenous solution. A PVA concentration 10 wt.% with respect to PLDLLA. Then, various content of PCCNWs (0, 0.1, 0.5, and 1 wt. % per PLDLLA weight) were added to the solution and stirred overnight at room temperature. The samples were named PLDLLA/PVA-X, where X represents the amount of PCCNWs. PLDLLA/PVA-X nanofibrous samples were developed using an electrospinning device (model eSpinner NF-CO EN/II, Asian Nanostructure Technology Co., Tehran, Iran) with voltage of 15 kV, syringe needle tip to collector distance of 18 cm, and the polymer solution flow rate of 0.4 mL. h^{-1}. The crosslinking of the nanofibrous samples was carried out by using glutaraldehyde solution (25% (v. v^{-1})) in a vacuum chamber at ambient temperature for 24 h followed by placing in in an oven at 45 ℃ for 24 h to remove the residuals. Further, the nanofibrous samples were exposed to the free air for 2 days to ensure that all of the residual solvents and unreacted crosslinking were evaporated.

2.4 CNWs yield calculation

CNWs yield (%) were calculated by using the following Eq.:

$$\text{Yield (\%)} = \frac{M_2}{M_1} \times 100 \quad (1)$$

Where "M_1" represents the mass of dried paper powder and "M_2" denotes the total mass of oven-dried CNWs.

2.5 X-ray fluorescence analysis

Chemical compositions of the wastepaper powder, CNWs, and PCCNWs were determined based on the X-ray fluorescence (XRF) method using a Philips Analytical XRF apparatus, Tehran, Iran.

2.6 Fourier transform infrared (FTIR) spectroscopy

An Attenuated total reflectance (ATR)-FTIR spectroscopy (model Equinox 55, Bruker Co., United States) with wavenumbers ranging 500–4000 cm^{-1} was used to identify the functional groups of of nanofibrous samples.

2.7 Water contact angle (WCA), water up-take capacity and hydrolytic degradation

hydrophilicity of PLDLLA/PVA nanofibrous with and without PCCNWs were evaluated by water contact angle (WCA) according to the Sessile drop method. The obtained angle demonstrates the wetness of water on the solid surface. A water droplet as dispersed on the samples surface, and WCA values were determined using a G-10 contact goniometer (Kruss, Germany). All experiments were carried out in triplicate.

The Water up-take capacity of nanofibrous samples was determined by tracking the weight before and after incubation in 50 mL buffer. Samples (0.06 mm in thickness, 50×50 mm^2 in surface area) were soaked in the 50 mL of phosphate buffer saline (PBS) at 37 °C, and taken out at different time point to measure the weight. The water up-take was calculated at the predetermined time intervals according to the following Eq:

$$\text{Water up-take (\%)} = \frac{W_t - W_0}{W_0} \times 100 \quad (2)$$

where "W_0" and "W_t" express the samples' weights before and after immersing into the PBS, respectively.

The remaining mass was measured to study the hydrolytic degradation of nanofibrous samples. PLDLLA/PVA-PCCNWs nanofibrous samples (weighed as M_i) were immersed in 50 mL of PBS at 37 °C. At specified time points, the samples were removed and placed in a vacuum chamber at 30 °C for 3 days, and weighted (M_f). The weight remaining ratio of nanofibrous samples were calculated according to the following Eq:

$$\text{Remaining mass (\%)} = \left(\frac{M_f}{M_i}\right) \times 100 \quad (3)$$

Where "M_i" is the initial weight of the samples and "M_f" is the weight of dried samples after degradation procedure. All experiments were carried out in triplicate

2.8 Field-emission scanning electron microscopy

the morphology of nanofibrous samples were investigated using field-emission scanning electron microscopy (FE-SEM; model NanoSEM 450, FEI Nova, Nebraska, USA). The samples were coated with a thin layer of gold to observation with high resolution. The average diameter of nanofibers was measured by utilizing ImageJ software.

2.9 Tensile test

The mechanical properties of PLDLLA/PVA-0, PLDLLA/PVA-0.1, PLDLLA/PVA-0.5, and PLDLLA/PVA-1 nanofibrous samples were assessed by a universal tensile apparatus (Instron, model 5566, Amersham, England) at crosshead speed of 5mm. min^{-1}. Elongation at break (E_b), ultimate tensile strength (UTS), and Young's modulus (E), were calculated in three independent experiments.

2.10 Cell culture and osteogenic differentiation

hMSCs and fibroblast cells (SNL76/7) obtained from the Stem Cell Technology Research Center (Tehran, Iran) were cultured in full cultured media i.e., Dulbecco's modified eagle medium (DMEM) supplemented with 10% fetal bovine serum (FBS), streptomycin sulfate (10 mg· mL^{-1}) and penicillin G sodium (10 units· mL^{-1}) under a humidified atmosphere containing 5% CO_2. Osteogenic induction of hMSCs

was performed by replacing the basal media with an osteogenic media containing DMEM supplemented with 10 % FBS, 10 nM dexamethasone, 50 mg. ml^{-1} ascorbic acid 2-phosphate, and 10 mM β-glycerophosphate. The cells were incubated at 37 ℃ and 5 % CO_2 for 14 days.

2.10.1 *Cell viability assay*

The cell viability, proliferation of fibroblast cells (SNL 76/7) treated by PLDLLA/PVA-0, PLDLLA/PVA0.1, PLDLLA/PVA-0.5, and PLDLLA/PVA-1 nanofibrous samples were evaluated by MTT assay[2]. The nanofibrous samples were placed in a 24-well culture plate and 1×10^4 cells/well were seeded and incubated at 37 °C with 5% of CO_2. The viability and proliferation of fibroblast cells (SNL 76/7) were determined after 1, 3, and 5 days of cell seeding. The cells were incubated in 10 mL 3-(4 dimethylthiazol-2-yl)-2, 5 diphenyl tetrazolium bromide, thiazolyl blue (MTT) solution (5 mg. mL^{-1}) for 4 h in 5% CO2 incubator at 37 °C. Then, the MTT solution was replaced by DMSO to dissolved dissolve the formazan crystals. The optical density of the nanofibrous samples were read using a microplate reader (BioTek Instruments Winooski, Vermont) (540–630 nm). The relative cell viability of the nanofibers was calculated by using Eq. (4).

$$\text{Relative cell viability (\%)} = \frac{OD}{avg\ ODC'} \times 100 \quad (4)$$

Where "OD" is the absorbance value of the experimental wells minus the zero wells and "$avg\ ODC'$ '" is the average absorbance value of the corrected control wells.

2.10.2 Cell attachments studies

FE-SEM micrograph imaging was used to investigate the adhesion and morphology of fibroblast cells (SNL 76/7) and hMSCs cultured on the nanofibrous samples after 1 day of cell culture. The samples were washed with PBS to removed non-adherent cells and fixed with glutaraldehyde 4% for 1 h. Then, they were rinsed with distilled water followed by dehydrating by A gradient of ethanol concentrations (20%, 30%, 50%, 70%, and 100%) for 10 min at each concentration to dry the samples.

2.10.3 Osteogenic differentiation and morphology of stem cells

Alkaline phosphatase (ALP) activity is an enzymatic marker to determine osteogenic differentiation on samples after cell culture at osteogenic induction media. The ALP activity of hMSCs cultured on nanofiber samples for 7 and 14 days were evaluated. The samples were washed three times with PBS, after 7, and 14 days of incubation in an osteogenic differentiation basal medium. 200 μL of radio immune precipitation analysis (RIPA) buffer was added to the cells utilized to extract entire proteins of wells. Then, cell suspensions were centrifuged at 15,000 g for 15 min at 4 °C. A microplate reader (BioTek Instruments, Winooski, Vermont) was used to determine the ALP activity (IUL^{-1}) against the total protein (mg) at 480 nm excitation and 520 nm emission.

Amount of calcium minerals deposited on nanofibrous samples were determined using a calcium assay kit (Parsazmun, Tehran, Iran). The cells was washed with PBS, and added 200 μL of HCL (0.6 mol. L^{-1}, Merck) and pipe taged were added to the wells for multiple times. The samples were shaken for 40 min at 4 °C, after transferring into vials. A calcium assay kit was used to determine the calcium deposit levels. An enzyme-linked immunosorbent assay (ELISA) reader apparatus was used to carry out the light absorbance at a wavelength of 570 nm. A standard concentration curve of serial dilutions of calcium against the corresponding to an optical density (OD) was used to determine calcium content.

Alizarin red staining shows osteogenic differentiation qualitatively that was carried out to indicate osteogenic differentiation of hMSCs on the nanofibrous samples. The cells on the nanofiber samples were fixed using formaldehyde solution 4 wt. % for 20 min and washed with PBS. Then, 0.5% Alizarin red was added to the wells and incubated for 5 min, and the samples were washed with distilled water. Finally, the stained bone cells were evaluated by light microscopy.

To study the morphology of hMSCs after 21 days of differentiation and compare the differences between the samples, FE-SEM was imaged with 10,000 x magnification.

2.11 Statistical analysis

Values are expressed as means ± standard error of the mean (SEM). Origin Lab 8 was used to perform statistical analyses by using two-way ANOVA followed by Bonferroni's post hoc test. The statistical significance of data was evaluated using $p < 0.05$ (*). All experiments were conducted three times.

3 Results and discussion

3.1 Preparation of PCCNW from cellulose microfibers

The preparation of PCCNWs from wastepaper is indicated in Fig. 1a. Briefly, shredded wastepaper fibers were hydrolyzed by phosphoric acid, which could break up the amorphous region and release crystallites[15]. The average diameter of microfibers was about 30µm containing both crystalline and amorphous areas. The amorphous regions were disappeared by acid hydrolysis and only crystalline parts remained, which called CNWs. Fig. 1(b, c) reveals optical and fluorescence microscopy images of cellulose microfibers of wastepaper. The CNWs were separated by a sonication [15]. The extracted CNWs yield was calculated, and it was about 37.9%. Finally, the acidic groups on CNWs, which can cause cell death, were replaced by calcium hydroxide (PCCNWs) (Fig. 1d). The PCCNWs have a length higher than 200nm and a diameter shorter than 10 nm. Therefore, their aspect ratio is $>$ 20, which can remarkably enhance the mechanical properties such as the tensile stress and Young's modulus of nanofibrous samples.

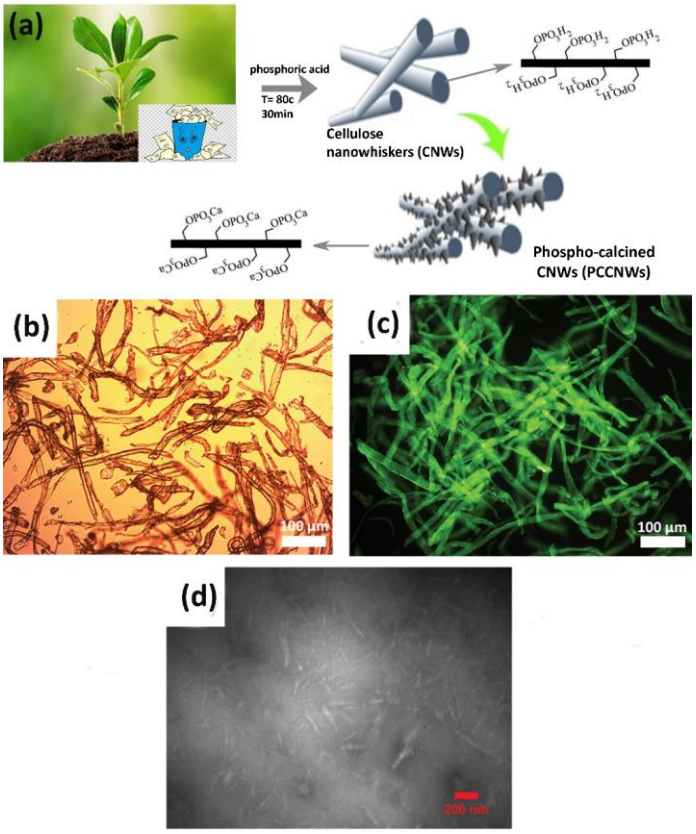

Fig. 1. (a) The preparation schematic of PCCNWs from wastepaper (b) Optical microscopy analysis of cellulose microfibers, (c) fluorescence microscopy analysis of cellulose microfibers and (d) TEM image of PCCNWs.

3.2 X-ray fluorescence study

X-ray fluorescence (XRF) analysis was carried out to evaluate and identify elements present in wastepaper, CNW, and PCCNW to show the difference between the calcified CNW with CNW (Table 1). The phosphorus group was present in the CNW (≅4.364±0.01 wt.%) and PCCNW (≅4.215±0.01 wt.%) chemical compositions. The calcium content in PCCNW chemical composition was more than the

chemical composition of the wastepaper and CNW that showed the calcium groups were placed on CNWs. In other words, the PCCNW had more calcium than wastepaper and CNW.

Table 1. XRF spectrometry results for the wastepaper, CNW, and PCCNW.

Sample	P_2O_5 (wt.%)	CaO (wt.%)	Fe_2O_3 (wt.%)	Na_2O (wt.%)	MgO (wt.%)	TiO_2 (wt.%)	MnO (wt.%)
Waste paper	0.02±0.01	0.110±0.01	0.437±0.01	0.003±0.01	N	0.013±0.01	0.01±0.011
CNW	4.364±0.01	0.114±0.01	0.435±0.01	0.001±0.01	N	0.013±0.01	0.012±0.01
PCCNW	4.215±0.01	12.043 ±0.01	0.438±0.01	0.11±0.01	0.400 ±0.01	0.013±0.01	0.013±0.01

3.3 Morphological observation

We prepared nanofibers from PLDLLA and PVA by electrospinning as a scaffold for bone tissue applications. Nanofibrous with a high surface area to volume can enhance cell adhesion and cell proliferation[17]. Moreover, the nanofibers provide a scaffold with high porosity that supports oxygen permeability and cell connectivity in the scaffold for the exchange of materials and signals [18]. Fig. 2(a-d) depicted the FE-SEM micrograph images of microfibrous samples such as PLDLLA/PVA-0 (Fig. 2a), PLDLLA/PVA-0.1 (Fig. 2b), PLDLLA/PVA-0.5 (Fig. 2c) and PLDLLA/PVA-1 (Fig. 2d). All samples revealed morphologies with uniformity, smoothness, and no beads. Moreover, by increasing the content of PCCNWs (0% to 1% per PLDLLA weight), the average diameter was increased from 227nm to 554nm (Fig. 2(a, d)). The average diameter only increased 20nm by adding 0.1% of PCCNWs to PLDLLA/PVA nanofibers, but with increasing content of PCCNWs from 0.1% to 0.5 and 1%, the nanofibrous average diameter significantly increased to 347nm and 554nm, respectively.

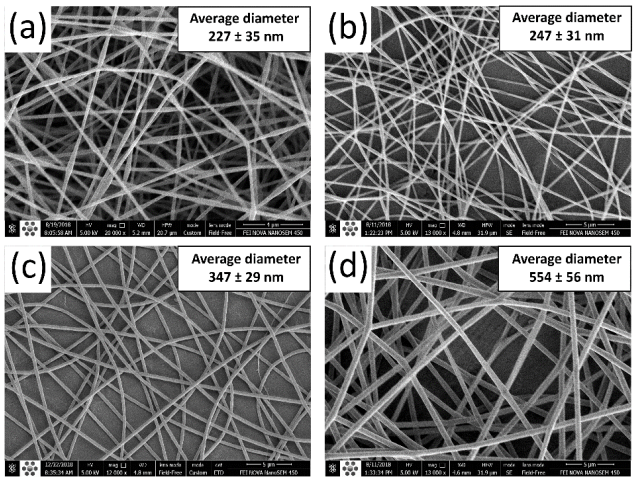

Fig. 2. FE-SEM micrograph images of (a) PLDLLA/PVA-0, (b) PLDLLA/PVA-0.1, (c) PLDLLA/PVA-0.5 and (d) PLDLLA/PVA-1 samples with scale bar of 5.0 micron.

3.4 Functional groups studies

The ATR-FTIR spectra of different functional groups of PVA, PLDLLA, PLDLLA/PVA and PLDLLA/PVA-1 samples are shown in table 2 and Fig. 3. The FTIR of PVA showed several characteristic bonds for O–H stretching (3319 cm^{-1}), C–H stretching (2938cm^{-1}), C=O stretching (1732 cm^{-1}), $–CH_2$ stretching (1428, 1373 cm^{-1}), C–O–C stretching (1247 cm^{-1}) and –C–O symmetric stretching (1089 cm^{-1}). The spectra of PLDLLA displayed some characteristic bonds at 2935, 2866 cm^{-1} (C–H stretching), 1750 cm^{-1} (C=O stretching), 1452, 1379 cm^{-1} ($–CH_2$ stretching), 1184 cm^{-1} (C–O–C stretching) and 1084 cm^{-1} (–C–O symmetric stretching). Although, by examining the ATR-FTIR spectra of the samples, it could be seen that no new peaks were appeared or disappeared in the PLA/PVA and PLA/PVA-1 samples in comparison with PLDLLA and PVA peaks, which indicated that no chemical reactions occurred between the two polymers, the characteristic peak some groups were shifted. For example, the characteristic peak of carbonyl groups and –C-O symmetric stretch for PLDLLA from 1750 cm^{-1} and 1084 cm^{-1} were shifted to 1755cm^{-1} and 1091

cm^{-1} for PLDLLA/PVA, respectively. Hydrogen bonds, dipole-dipole, and other physical interactions can transfer the wavenumbers of bonds to other wavenumbers[11]. Hence, can be concluded that PLDLLA and PVA had the physical interactions. Although, between the characteristic peaks of PLDLLA/PVA and PLDLLA/PVA samples do not had significant difference, the alteration in wavenumbers of some groups were seen. The characteristic peaks of PLDLLA/PVA-1 such as C=O stretching, -C-O symmetric stretching, and O-H stretching were shifted to lower wavenumbers compared to PLDLLA/PVA-1 samples (Table 2). The content of PCCNWs (1 wt.%) and PVA (10 wt.%) was slight in the samples so it could be the reason for minor changes. Further to the alteration at wavenumbers, the intensity of peaks was decreased, which is due to the formation of hydrogen bonds between PCCNWs and PVA[19]. Related to these observations, some similar works have been reported in the literature [3, 20].

Table 2. The ATR-FTIR peaks assignments of functional groups for PLDLLA, PVA, PLDLLA/PVA, and PLDLLA/PVA-1 nanofibrous samples.

	PLDLLA	PVA	PLDLLA/PVA	PLDLLA/PVA-1
Assignments	Position (cm^{-1})	Position (cm^{-1})	Position (cm^{-1})	Position (cm^{-1})
$O-H$		3319	3326	3317
$C-H\ stretching$	2935,2866	2938	2992,2943	2974,2920
$C=O$	1750	1732	1755	1747
$-CH_2$	1452,1379	1428,1373	1452,1377	1451,1378
$-C-O-C-$	1184	1247	1188	1187
$-C-O$ $symmetric\ stretch$	1084	1089	1091	1088

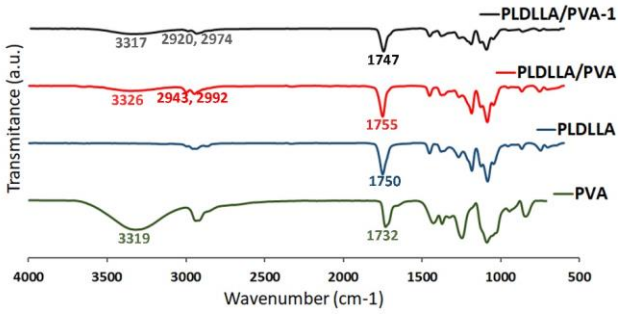

Fig. 3. ATR-FTIR spectra of PVA, PLDLLA, PLDLLA/PVA and PLDLLA/PVA-1 samples.

3.5 Mechanical properties

Table 3 shows the tensile results of PLDLLA/PVA-0, PLDLLA/PVA-0.1, PLDLLA/PVA-0.5, and PLDLLA/PVA-1 samples. The increase of PCCNWs content led to an improvement in the tensile stress of samples. Maximum stress was 24.3±0.9 MPa which occurred at 0.5 wt.% PCCNWs loading, and then it was lowered. The reduction of tensile stress of PLDLLA/PVA-1 compared to PLDLLA/PVA-0.5 was due to defect phenomenon that was meant an increase in the number of PCCNWs as an impurity in the PLDLLA/PVA matrix [2, 21]. In other words, this reduction could due to agglomeration of PCCNWs at higher concentrations and making weak positions in the nanofibrous mats, which could act as stress concentration points. This trend was also presented in some earlier published works [3, 20, 22]. Moreover, the maximum and minimum tensile strain for PLDLLA/PVA-0 and PLDLLA/PVA-1 are 40±2.1% and 25±1.2%, respectively. The tensile modulus increased through the enhancing of PCCNWs also revealed the reinforcement influence of the PCCNWs on the PLDLLA/PVA matrix, which could be due to high surface area and high elastic modulus of PCCNWs as well as the hydrogen bonds between PCCNWs and PVA. The lowest and highest modulus of 324±9 MPa and 464±7 MPa occurred for PLDLLA/PVA-0 and PLDLLA/PVA-

1 samples, respectively. In a case study, Li *et al.* [23] compared mechanical behavior of uncoated and CNWs coated 45S5 bioactive glass scaffolds and their results showed that presence of CNWs improve the tensile strength of the scaffolds from 0.02 MPa to 0.06 MPa and made the scaffolds much tougher. Consequently, the strength of scaffolds was improved by increasing the CNWs amount in nanocomposites used for bone tissues.

Table 3. The mechanical properties of PLDLLA/PVA-0, PLDLLA/PVA-0.1, PLDLLA/PVA-0.5 and PLDLLA/PVA-1 samples.

Sample	Tensile stress ± SD (MPa)	Tensile strain ± SD (%)	Young's modulus ± SD (MPa)
PLDLLA/PVA-0	17±0.5	40±2.1	324±9
PLDLLA/PVA-0.1	18.8±0.8	32±1.5	374±11
PLDLLA/PVA-0.5	24.3±0.9	28±1	420±5
PLDLLA/PVA-1	22.8±0.5	25±1.2	464±7

3.6 Water contact angle (WCA), water up-take, and hydrolytic degradation

To enhance tendency of cells for adhesion, the hydrophilicity of scaffolds is an essential factor [1, 24]. Fig. 4a shows the WCA of all samples. By addition of different amount of PCCNWs to the PLDLLA/PVA matrix, the contact angle values decreased from 65° for PLDLLA/PVA-0 to 56° for the PLDLLA/PVA-1, respectively due to the hydrophilic nature of cellulose. The amount of water up-take of the nanofibrous nanocomposite samples was illustrated in Fig. 5b. This value was increased by increasing of PCCNWs content in composition due to the hydrophilicity enhancement of samples. The PLDLLA/PVA-1 sample showed the highest amount of water up-take (82%, see Fig. 4b).

Moreover, hydrophilicity and water up-take impress directly on degradation. Fig. 4c depicted the hydrolytic degradation of PLDLLA/PVA-PCCNWs nanofibrous samples, which were carried out in PBS with a pH of 7.4 at 37°C during a 42-day period. Ester bonds in the backbone of PLA are broken via water molecules in aqueous media and the rate of PLA hydrolytic degradation is controlled by inherent properties and degradation environment conditions. The inherent features such as molecular weight, the structure of the backbone, absorbed water, and crystallinity. The chain fragment diffusion coefficient within the polymer, the degradation product solubility, the rate constant, pH, and temperature of degradation media are effective conditions[25]. In general, PLA matrices in aqueous media can proceed through surface or heterogeneous reaction or/and bulk or homogeneous erosion[25, 26]. The hydrolytic degradability of the nanofibrous samples was accelerated with enhancing the PCCNWs content and the highest amount of hydrolytic degradation for PLDLLA/PVA-1 is 48.4%. In our previous work, the WCA of PLA nanofibers was 120°, as is seen in Fig. 4a the WCA of PLDLLA/PVA is 65°, which shows 10% PVA significantly improves the hydrophilicity of the system, which is an essential factor in tissue engineering. Further, as is said, the hydrophilicity of nanofibrous samples was increased by increasing the PCCNWs content. By comparing the remaining mass of PLDLLA nanofibers with PLDLLA/PVA and PLDLLA/PVA-X nanofibers samples, it is obvious that the presence of PVA and PCCNWs simultaneously accelerated the hydrolytic degradation of PLDLLA nanofibers.

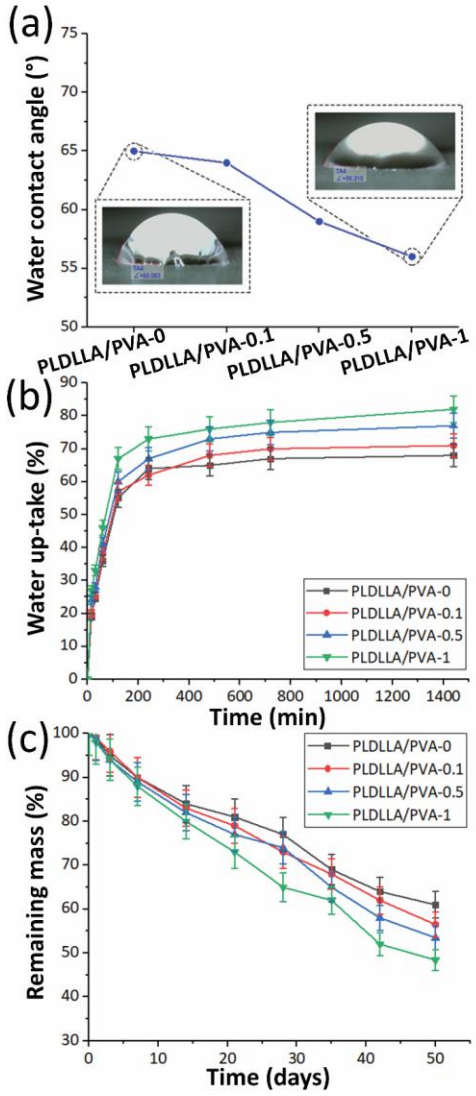

Fig. 4. (a) Water contact angle, (b) water up-take and (c) remaining mass in PBS solution for PLDLLA/PVA-0, PLDLLA/PVA-0.1, PLDLLA/PVA-0.5 and PLDLLA/PVA-1 samples.

3.7 Cytotoxicity and cell attachment

The fibroblast cells (SNL 76/7) were cultured on TCPS, PLDLLA/PVA-0, PLDLLA/PVA-0.1, PLDLLA/PVA-0.5, and PLDLLA/PVA-1 nanofibrous samples and the cytotoxicity and cell viability of them after 1, 3, and 5 days were studied (Fig. 5.). The nanofibrous scaffolds with various content of PCCNWs had greater cell viability than the control samples (TCPS) during assay time. By increasing the percentage of PCCNWs the hydrophilicity of samples increased. This more hydrophilicity increased tendency of fibroblast cell for adhesion as a result more proliferated cells[17, 27]. However, the cytotoxicity and cell viability values of PLDLLA/PVA-PCCNWs nanofibrous samples showed no significant difference with control sample, which can be concluded that they have no cytotoxicity [3, 21]. In general, cell viability values are classified in four groups including severe, moderate, slight and not cytotoxic with values of <30%, between 30 and 60%, between 60 and 90% and >90%, respectively [28]. The results indicated that all PLDLLA/PVA-PCCNWs samples were associated with cell viabilities above 90%.

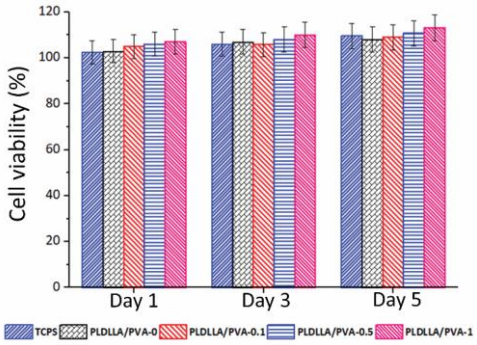

Fig. 5. Cell viability in response to PLDLLA/PVA-PCCNWs scaffolds treatment. SNL76/7 cells were treated for 1, 3 and 5 days in the absence or presence of PLDLLA/PVA-PCCNWs scaffolds with various PCCNWs concentration (0, 0.1, 0.5 1wt.% per PLDLLA). Results are expressed as % of cell viability and are the mean ± SEM of three independent experiments. Data were analyzed using two-way ANOVA tes**t.**

Generally, scaffolds are able to show good cell adhesion and following that more proliferation that provides an environment like ECMs. Two factors that help the scaffolds in this way are hydrophilicity and porous structure[25]. Fig. 6(a–d) depicted the FE-SEM micrograph images of fibroblast cells (SNL76/7) adhesion after 1 day of seeding on PLDLLA/PVA-0 (Fig. 6a), PLDLLA/PVA-0.1 (Fig. 6b), PLDLLA/PVA-0.5 (Fig. 6c) and PLDLLA/PVA-1 (Fig. 6d). By increasing PCCNWs content from 0 to 1%, the tendency of cells to adhesion on scaffolds increased and the PLDLLA/PVA-1 sample showed the best cell morphology and growth area among others (see Fig. 6 (a-d)). These findings could be related to an increase in hydrophilicity as well as biocompatibility of samples. In a case study, Rashtchian *et al*. [29] compared cell attachment morphologies of PCL-PVA/ NaAlg and PCL-CaAlg nanofibers with and without cellulose nanocrystals (CNC) and their results showed that fibroblast cells displayed more efficient cell adhesion and expansion on the samples containing CNC than on CNC-free samples due to enhancement of hydrophilicity. To evaluate the cell proliferation on nanofibrous samples, after 3 and 5 days of cell seeding the FE-SEM micrograph images of fibroblast cells (SNL76/7) on PLDLLA/PVA-1 was carried out for example (Fig. 6 (e and f)). The proliferation of fibroblast cells on PLDLLA/PVA-1 nanofibers were observed at day 5 of cell seeding, the cells have well attached to the nanofibers scaffold and they have become widespread on PLDLLA/PVA-1 nanofibers sample.

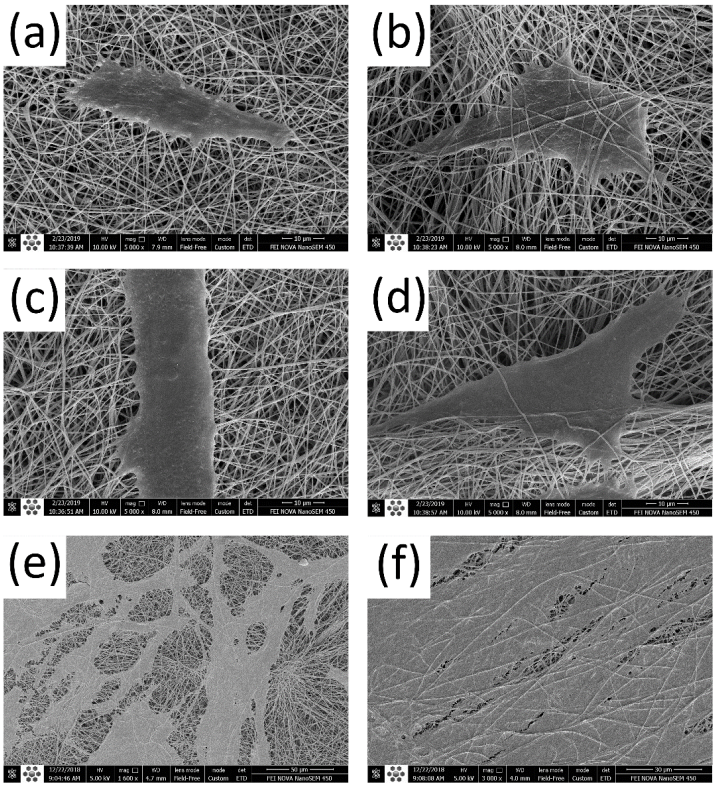

Fig. 6. FE-SEM micrograph images of fibroblast cells (SNL76/7) adhesion after 1 day of seeding on (a) PLDLLA/PVA-0, (b) PLDLLA/PVA-0.1, and (c) PLDLLA/PVA-0.5, as well as FE-SEM micrograph images of fibroblast cells (SNL76/7) adhesion on PLDLLA/PVA-1 after 1 day (d), 3 days (e), and 5 days (f).

3.8 Assessment of osteogenic markers

The produced osteogenic differentiation arising from scaffolds and osteogenic medium are investigate and evaluate by alkaline phosphatase (ALP), osteocalcin (OCN),collagen I and runt-related transcription factor 2 (Runx2), and bone sialoprotein that are differentiation markers [30].

3.8.1 Alkaline phosphatase activity (ALP)

The ALP activity is widely known as an early osteogenic differentiation marker. Fig. 7a depicts osteogenic differentiation of hMSCs on PLDLLA/PVA-PCCNWs after 7 and 14 days. The nanofibers due to the high specific surface area and structure similar to the ECM can show better cell attachment and proliferation. Another factor effective on cell adhesion and proliferation is surface hydrophilicity of sacaffolds. Hence, the PLDLLA/PVA-PCCNWs nanofibrous scaffolds, which had good hydrophilicity and morphology like ECMs, revealed more cell proliferation than TCPS. Therefore, more cell proliferation means the more number of cells that can produce enzymes that led to higher ALP activity for PLDLLA/PVA-PCCNWs samples compared to TCPS. Moreover, by increasing the PCCNWs content in the blend PLDLLA/PVA nanofibers, the hydrophilicity of them was enhanced and consequently, the ALP activity was improved from 0.16 for PLDLLA/PVA-0 to 0.233 for PLDLLA/PVA-1 nanofibrous samples (Fig. 7a). As is seen in Fig. 7a, PLDLLA/PVA-1 had a significant difference compared to other nanofibrous samples and TCPS so that the ALP activity of PLDLLA/PVA-1 nanofibers scaffold was 1.6 times higher than the ALP activity of TCPS. This increase in the ALP activity not only is due to the good hydrophilicity but also can due to the functional groups on PCCNWs. Calcium phosphate and phosphate groups on surface of CNWs can play a role like hydroxyapatite and increase the osteogenic differentiation. Moreover, morphology like ECM, good hydrophilicity, porosity, and possessing the mechanical properties required to bone tissue of nanofibrous scaffolds are other factors that can induce better osteogenic differentiation. The effect of morphology (nanofibers) and PVA (hydrophilicity) on the ALP activity can be seen by comparing the ALP of TCPS and PLDLLA/PVA-0, which shows the hydrophilic nanofibers are able to produce more enzymes.

3.8.2 Calcium content assay

Step two in the differentiation process of hMSCs is creation of mineral on themselves by passing the time from cell seeding [24]. Therefore, mineral deposits were determined on the nanofibrous samples by calculation of calcium deposition in differentiated hMSCs on days 7 and 14 after osteogenic induction.

Fig. 7b illustrates the mineral deposits on the PLDLLA/PVA-PCCNWs scaffolds. A similar trend like the ALP activity was observed for calcium content. The PLDLLA/PVA-0 nanofibers scaffold had better calcium content compared to TCPS at 7 and 14 days could be due to the inherent potential of nanofibers in mimicking ECM for cells and the hydrophilicity caused by PVA. By increasing the content of PCCNWs from 0 wt.% to 1 wt.% in PLDLLA/PVA nanofibrous samples, the calcium content was increased from 0.263 (μg/scaffold) to 0.359 (μg/scaffold) after 14 days (Fig. 7b). As is seen, the calcium phosphate and phosphate groups on PCCNWs can mimic hydroxyapatite role and increase the ostegenic differentiation of hMSCs. In a case study, Jafari *et al*. [2] developed PCL scaffolds containing of 0.1 and 0.5 wt.% of phospho-calcified CNWs revealed much higher ALP activity and calcium content than to TCPS after passing 7 and 14 days of incubation in osteogenic differentiation medium. According to the ALP activity and calcium content results, the PLDLLA/PVA nanofibers scaffold had a good performance in bone tissue engineering but by adding PCCNWs its performance enhanced so that the PLDLLA/PVA-1 scaffold showed the best efficiency.

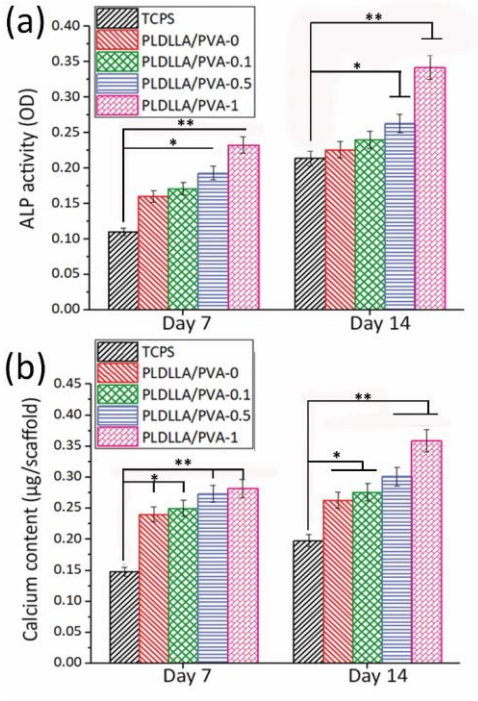

Fig. 7. The osteogenic mineralization analysis of two group samples is shown. (a) ALP analysis of hMSCs ($p < 0.05$) and (b) The measured optical density levels of calcium minerals deposited by hMSCs due to osteogenic induction. Results are expressed as % of ALP activity (OD), and calcium content (µg/scaffold) and are the mean ± SEM of three independent experiments. Data were analyzed using two-way ANOVA test. *$p < 0.05$; **$p < 0.005$; as compared to the control.

3.8.3 Alizarin red staining

Alizarin red staining is an applicable method for marking mineralization during osteogenic differentiation. Calcified cells appear with red color in alizarin red staining as mark as mineralization during osteogenic differentiation. The same light intensity of alizarin red staining on TCPS (Fig. 8a), PLDLLA/PVA-0 (Fig. 8b), PLDLLA/PVA-0.1 (Fig. 8c), PLDLLA/PVA-0.5 (Fig. 8d) and PLDLLA/PVA-1 (Fig. 8e) after 14 days of incubation in osteogenic medium was carried out. As shown, the calcium deposition on the scaffolds that

staining by alizarin red was higher than TCPS (intensity of red color). In a research work, Shahrousvand *et al*. [3] performed alizarin red staining of osteogenic differentiated hMSCs on the polyurethane (PU)- Poly (2 hydroxyethyl methacrylate) (PHEMA)- poly(caprolactone) (PCL) scaffolds containing different amount of CNWs (0% to 1%) after 14 days incubation in osteogenic medium and concluded that calcium deposition by alizarin red staining was increased by increasing CNWs content in scaffolds.

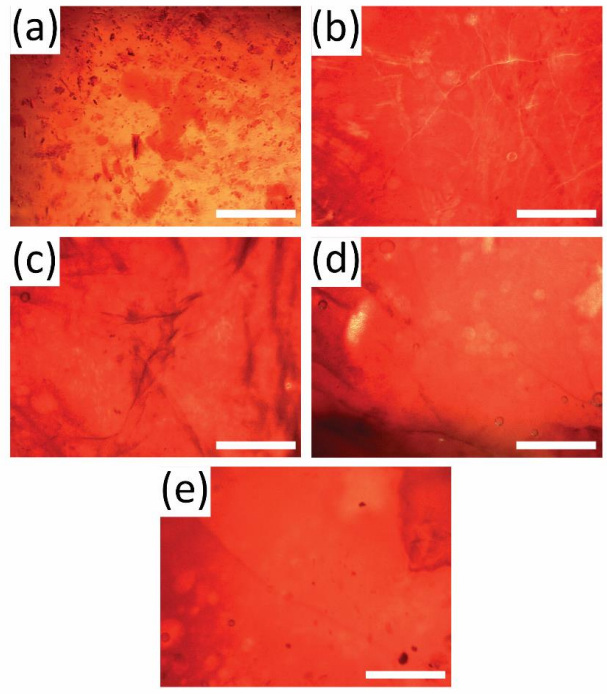

Fig. 8. Alizarin red staining of osteogenic differentiation of hMSCs is shown. hMSCs cultured onto (a) TCPS, (b) PLDLLA/PVA-0, (c) PLDLLA/PVA-0.1, (d) PLDLLA/PVA-0.5 and (e) PLDLLA/PVA-1 after 14 days (scale bar: 100 µm).

3.8.4 Morphology of hMSCs after differentiation

The FE-SEM images of hMSCs on PLDLLA/PVA-PCCNW nanofibrous scaffolds after 14 days of incubation in the differentiation media are shown in Fig. 9(a-d). By increasing the PCCNWs content (0% to

1%), proliferation of differentiated cells was spread and attached to the PLDLLA/PVA-PCCNWs scaffolds more and mineral deposits were better defined on them.

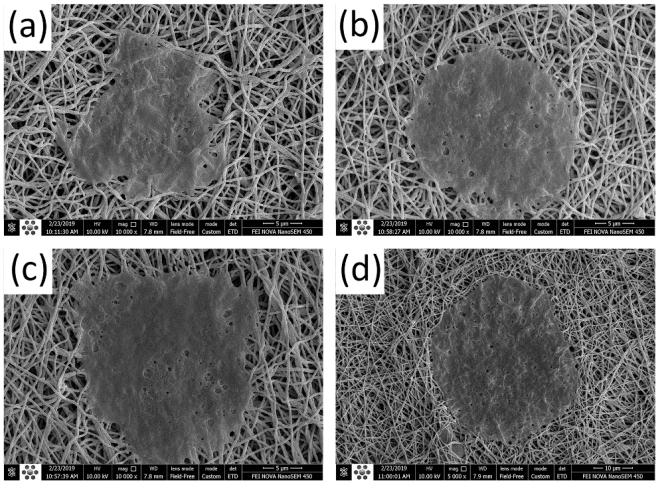

Fig. 9. FE-SEM micrograph images of hMSCs adhered on PLDLLA/PVA-PCCNWs scaffolds after 14 days' incubation in osteogenic differentiation medium: (a) PLDLLA/PVA-0, (b) PLDLLA/PVA-0.1, (c) PLDLLA/PVA-0.5 and (d) PLDLLA/PVA-1.

4 Conclusion

To achieve a scaffold with high performance in bone tissue engineering, PLDLLA was blended with 10 wt.% PVA to enhance its hydrophilicity and accelerate its degradation rate. PCCNWs were prepared from wastepaper followed by surface modification to incorporate calcium and phosphate groups for osteogenic differentiation and incorporated with various concentrations (0, 0.1, 0.5, and 1%) in the PLDLLA/PVA blend. All nanofibrous samples showed a good performance as a bone scaffold but the PLDLLA/PVA-1 nanofibers scaffold had the best efficiency compared to the others. The water contact angle and ultimate water up-take of PLDLLA/PVA-1 were 56° and 82%, respectively. The fastest hydrolytic degradation belonged to the PLDLLA/PVA-1 nanofibers. Although by increasing the PCCNWs from 0 to 1% Young's

modulus increased from 324 to 464 MPa, the tensile strain showed a decreasing trend. Cytotoxicity of samples was revealed by MTT assay and no toxic was observed. According to the results of ALP activity, calcium content, and alizarin red staining, as osteogenic differentiation markers, the PLDLLA/PVA-PCCNWs nanofibrous scaffold could support proliferation and differentiation of hMSCs. The PLDLLA/PVA-1 had the best results compared to the other samples and can provide new nanocomposite for bone tissue engineering application.

References

[1] P. Ghaffari-Bohlouli, P. Zahedi, M. Shahrousvand, Enhanced osteogenesis using poly (l-lactide-co-d, l-lactide)/poly (acrylic acid) nanofibrous scaffolds in presence of dexamethasone-loaded molecularly imprinted polymer nanoparticles, International Journal of Biological Macromolecules 165 (2020) 2363-2377.

[2] H. Jafari, M. Shahrousvand, B. Kaffashi, Reinforced poly (ε-caprolactone) bimodal foams via phospho-calcified cellulose nanowhisker for osteogenic differentiation of human mesenchymal stem cells, ACS Biomaterials Science & Engineering 4(7) (2018) 2484-2493.

[3] M. Shahrousvand, M. Ghollasi, A.A.K. Zarchi, A. Salimi, Osteogenic differentiation of hMSCs on semi-interpenetrating polymer networks of polyurethane/poly (2-hydroxyethyl methacrylate)/cellulose nanowhisker scaffolds, International journal of biological macromolecules 138 (2019) 262-271.

[4] S. Shrestha, B.K. Shrestha, S.W. Ko, R. Kandel, C.H. Park, C.S. Kim, Engineered cellular microenvironments from functionalized multiwalled carbon nanotubes integrating Zein/Chitosan@ Polyurethane for bone cell regeneration, Carbohydrate Polymers 251 (2021) 117035.

[5] S. Gautam, C. Sharma, S.D. Purohit, H. Singh, A.K. Dinda, P.D. Potdar, C.-F. Chou, N.C. Mishra, Gelatin-polycaprolactone-nanohydroxyapatite electrospun nanocomposite scaffold for bone tissue engineering, Materials Science and Engineering: C 119 (2021) 111588.

[6] P. Naderi, M. Zarei, S. Karbasi, H. Salehi, Evaluation of the effects of keratin on physical, mechanical and biological properties of poly (3-hydroxybutyrate) electrospun scaffold: Potential application in bone tissue engineering, European Polymer Journal 124 (2020) 109502.

[7] L. Rojas-Martínez, C. Flores-Hernandez, L. López-Marín, A. Martinez-Hernandez, S. Thorat, C.R. Vasquez, A. Del Rio-Castillo, C. Velasco-Santos, 3D printing of PLA composites scaffolds reinforced with keratin and chitosan: Effect of geometry and structure, European Polymer Journal 141 (2020) 110088.

[8] T.-Y. Lu, W.-C. Huang, Y. Chen, N. Baskaran, J. Yu, Y. Wei, Effect of varied hair protein fractions on the gel properties of keratin/chitosan hydrogels for the use in tissue engineering, Colloids and Surfaces B: Biointerfaces 195 (2020) 111258.

[9] B. Ashwin, B. Abinaya, T. Prasith, S.V. Chandran, L.R. Yadav, M. Vairamani, S. Patil, N. Selvamurugan, 3D-poly (lactic acid) scaffolds coated with gelatin and mucic acid for bone tissue engineering, International journal of biological macromolecules 162 (2020) 523-532.

[10] Poly(Lactic Acid), Bio-Based Plastics2013, pp. 171-239.

[11] P. Ghaffari-Bohlouli, F. Hamidzadeh, P. Zahedi, M. Shahrousvand, M. Fallah-Darrehchi, Antibacterial nanofibers based on poly (l-lactide-co-d, l-lactide) and poly (vinyl alcohol) used in wound dressings potentially: A comparison between hybrid and blend properties, Journal of Biomaterials Science, Polymer Edition 31(2) (2020) 219-243.

[12] M. Sheth, R.A. Kumar, V. Davé, R.A. Gross, S.P. McCarthy, Biodegradable polymer blends of poly (lactic acid) and poly (ethylene glycol), Journal of applied polymer science 66(8) (1997) 1495-1505.

[13] H.W. Kim, H.S. Yu, H.H. Lee, Nanofibrous matrices of poly (lactic acid) and gelatin polymeric blends for the improvement of cellular responses, Journal of Biomedical Materials Research Part A: An Official Journal of The Society for Biomaterials, The Japanese Society for Biomaterials, and The Australian Society for Biomaterials and the Korean Society for Biomaterials 87(1) (2008) 25-32.

[14] A.-M. Haaparanta, E. Järvinen, I.F. Cengiz, V. Ellä, H.T. Kokkonen, I. Kiviranta, M. Kellomäki, Preparation and characterization of collagen/PLA, chitosan/PLA, and collagen/chitosan/PLA hybrid scaffolds for cartilage tissue engineering, Journal of Materials Science: Materials in Medicine 25(4) (2014) 1129-1136.

[15] M. Shahrousvand, F.A. Tabar, E. Shahrousvand, A. Babaei, M.M. Hasani-Sadrabadi, G.M.M. Sadeghi, H. Jafari, A. Salimi, High aspect ratio phospho-calcified rock candy-like cellulose nanowhiskers of wastepaper applicable in osteogenic differentiation of hMSCs, Carbohydrate polymers 175 (2017) 293-302.

[16] S. Samavedi, A.R. Whittington, A.S. Goldstein, Calcium phosphate ceramics in bone tissue engineering: a review of properties and their influence on cell behavior, Acta biomaterialia 9(9) (2013) 8037-8045.

[17] P. Ghaffari-Bohlouli, M. Shahrousvand, P. Zahedi, M. Shahrousvand, Performance evaluation of poly (l-lactide-co-d, l-lactide)/poly (acrylic acid) blends and their nanofibers for tissue engineering applications, International journal of biological macromolecules 122 (2019) 1008-1016.

[18] K. Balagangadharan, S. Dhivya, N. Selvamurugan, Chitosan based nanofibers in bone tissue engineering, International journal of biological macromolecules 104 (2017) 1372-1382.

[19] Z. Jahan, M.B.K. Niazi, Ø.W. Gregersen, Mechanical, thermal and swelling properties of cellulose nanocrystals/PVA nanocomposites membranes, Journal of industrial and engineering chemistry 57 (2018) 113-124.

[20] H. Jafari, M. Shahrousvand, B. Kaffashi, Preparation and characterization of reinforced poly (ε-caprolactone) nanocomposites by cellulose nanowhiskers, Polymer Composites 41(2) (2020) 624-632.

[21] M. Shahrousvand, M.S. Hoseinian, M. Ghollasi, A. Karbalaeimahdi, A. Salimi, F.A. Tabar, Flexible magnetic polyurethane/Fe2O3 nanoparticles as organic-inorganic nanocomposites for biomedical applications: Properties and cell behavior, Materials Science and Engineering: C 74 (2017) 556-567.

[22] A. Hivechi, S.H. Bahrami, R.A. Siegel, Drug release and biodegradability of electrospun cellulose nanocrystal reinforced polycaprolactone, Materials Science and Engineering: C 94 (2019) 929-937.

[23] W. Li, N. Garmendia, U.P. de Larraya, Y. Ding, R. Detsch, A. Grünewald, J.A. Roether, D.W. Schubert, A.R. Boccaccini, 45S5 bioactive glass-based scaffolds coated with cellulose nanowhiskers for bone tissue engineering, RSC advances 4(99) (2014) 56156-56164.

[24] M. Shahrousvand, G.M.M. Sadeghi, A. Salimi, The superficial mechanical and physical properties of matrix microenvironment as stem cell fate regulator, Advanced Surfaces for Stem Cell Research 23 (2016) 23.

[25] M.A. Elsawy, K.-H. Kim, J.-W. Park, A. Deep, Hydrolytic degradation of polylactic acid (PLA) and its composites, Renewable and Sustainable Energy Reviews 79 (2017) 1346-1352.

[26] J. Siepmann, N. Peppas, Mathematical modeling of controlled drug delivery, Advanced drug delivery reviews 48(2-3) (2001).

[27] S.M. Nalluri, G.R. Krishnan, C. Cheah, A. Arzumand, Y. Yuan, C.A. Richardson, S. Yang, D. Sarkar, Hydrophilic polyurethane matrix promotes chondrogenesis of mesenchymal stem cells, Materials Science and Engineering: C 54 (2015) 182-195.

[28] E.-C. Lönnroth, Toxicity of medical glove materials: a pilot study, International Journal of Occupational Safety and Ergonomics 11(2) (2005) 131-139.

[29] M. Rashtchian, A. Hivechi, S.H. Bahrami, P.B. Milan, S. Simorgh, Fabricating alginate/poly (caprolactone) nanofibers with enhanced bio-mechanical properties via cellulose nanocrystal incorporation, Carbohydrate Polymers 233 (2020) 115873.

[30] M. Terauchi, T. Inada, A. Tonegawa, A. Tamura, S. Yamaguchi, K. Harada, N. Yui, Supramolecular inclusion complexation of simvastatin with methylated β-cyclodextrins for promoting osteogenic differentiation, International journal of biological macromolecules 93 (2016) 1492-1498.